Feedback force and velocity control of an arm exoskeleton to assist user motion

Thang Cao Nguyen[1], Tuan Ngoc Nguyen[2]
[1]Institute of Mechanics, Vietnam Academy of Science and Technology, Hanoi, Vietnam
[2]Graduate School of Science and Technology, Vietnam Academy of Science and Technology, Hanoi, Vietnam
[1]Corresponding author
E-mail: [1]*caothangnguyen@imech.vast.vn*, [2]*ntngoc@freyssinet.com.vn*

Received 6 January 2024; accepted 19 February 2024; published online 2 March 2024
DOI https://doi.org/10.21595/mme.2024.23915

Abstract. The paper proposes a feedback force and velocity control of an arm exoskeleton to assist user motion. The original published control so-called feedback hybrid force and position control was based on the force and position control and was designed to assist user motion. This original control was successful at providing assist for the user's arm. This article presents an improved control scheme called the feedback force and velocity control. The proposed control is designed to regulate the velocities of joints of the exoskeleton and the feedback forces on links to assist user motion. The design and optimization of the feedback force and velocity control are realized by the Balancing Composite Motion Optimization (BCMO). The numerical method is realized in the paper to show that the proposed control is better than the original control in terms of less oscillation and fast response.

Keywords: arm exoskeleton, feedback force control, velocity control, optimal, modelling, simulation.

1. Introduction

The paper proposes an arm exoskeleton that can be worn on the human arm, can operate under the control of the user to move in the vertical direction Oz and horizontal direction Ox, Oy and has the ability to provide forces to assist the user motion. We use force sensors in the exoskeleton robot for sensing the feedback forces, and we use actuators for actuating joints. The overviews of the arm exoskeleton robots were introduced in [1-4], and the force control method was developed in [5-9]. The force control is generalized to regulate the feedback force in [10], [11], and [18]. Recently the feedback hybrid force and position control method for assisting the user motion has been published in [12]. Although the force control was successful at controlling all the feedback forces on links, it contained many oscillations and errors. In the other force control design [6], there was a velocity regulator for regulating the angular velocities of joints. The velocities of joints were regulated base on the measured feedback forces. This velocity regulator achieved the desired performances in terms of fast response and less oscillation. In this paper, a feedback force and velocity control is proposed to regulate the velocities of joints of the exoskeleton and the feedback forces on links. The proposed control aims to improve the original control in terms of fast response and less oscillation. A scenario is proposed with two phases [11], [12].

– Phase 1: the user actively exerts forces to signal the arm exoskeleton to generate desired velocities.

– Phase 2: the arm exoskeleton regulates the actuators at joints of the arm exoskeleton to assist the user motion.

The arm exoskeleton makes the following steps: The angles and angular velocities of the joints are ultilized to generalize the desired feedback forces on links while the feedback interaction forces on links are exploited to generalize the desired velocities of links. For assisting the user motion with desired velocities, the proposed arm exoskeleton actuates joints to regulate the feedback forces on the links and the velocities of joints.

The feedback force and velocity control is optimized by using the BCMO [14]. The numerical simulation is realized to show that the proposed arm exoskeleton has achieved the desired performances in terms of less oscillation and fast response.

2. Arm exoskeleton design

An arm exoskeleton is modelled in the Fig. 1. The arm exoskeleton possesses four joints θ_1, θ_2, θ_3, θ_4 including two joints at the shoulder θ_1, θ_2, a joint at the elbow θ_3, and a joint at the wrist θ_4. It has four links a_1, a_2, a_3, a_4 including two shoulder links a_1, a_2, one elbow link a_3 and one wrist link a_4. The masses of four links 1, 2, 3, 4 are represented by m_1, m_2, m_3, m_4, respectively. The feedback forces between user and the exoskeleton on the links are F_1, F_2, F_3, F_4. The distance between the vector of forces F_1, F_2, F_3, F_4 on the links and the center lines of joints are l_1, l_2, l_3, l_4. The arm exoskeleton possesses four controlled torques u_{M_1}, u_{M_2}, u_{M_3}, u_{M_4} at fours joints. The torques at revoluted joints are actuated by the servo motors to support the user.

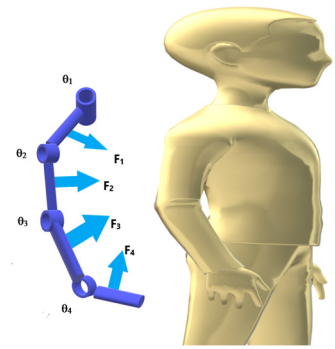

Fig. 1. A model of a 4-DOF arm exoskeleton and user

The Denavite-Hartenberge (D-H) table is provided in Table 1.

Table 1. The D-H table

Link	a	α	d	θ
1-1	0	$\frac{\pi}{2}$	0	$\theta_1+\frac{\pi}{2}$
1-2	0	0	a_1	0
2	a_2	0	0	$\theta_2-\frac{\pi}{2}$
3	a_3	0	0	θ_3
4-1	a_4	$-\frac{\pi}{2}$	0	θ_4
4-2	0	0	0	$-\frac{\pi}{2}$

From the D-H table, the individual homogeneous transformation matrices are obtained by Eq. (1), [15]:

$$A_i^{i-1} = Rot(z,\theta_i)Trans(0,0,d_i)Rot(x,\alpha_i)Trans(a_i,0,0) = \begin{bmatrix} \cos\theta_i & -\sin\theta_i\cos\alpha_i & \sin\theta_i\sin\alpha_i & a_i\cos\theta_i \\ \sin\theta_i & \cos\theta_i\cos\alpha_i & -\cos\theta_i\sin\alpha_i & a_i\sin\theta_i \\ 0 & \sin\alpha_i & \cos\alpha_i & d_i \\ 0 & 0 & 0, & 1 \end{bmatrix}. \quad (1)$$

The homogeneous transformation matrix of the end effector is calculated as follows:

ISSN PRINT 2351-5279, ISSN ONLINE 2424-4627

$$A_4^0 = A_1^0 A_2^1 A_3^2 A_4^3. \quad (2)$$

3. Feedback force and velocity control

The arm exoskeleton is controlled by the Eq. (3) [6], [12], [16]. The torques at revoluted joints are actuated by the servo motors and the user:

$$M(\theta)\xi + C(\theta,\omega) + G(\theta) + D(\omega) = u_M + u_H, \quad (3)$$

where, $\theta = [\theta_1 \quad \theta_2 \quad \theta_3 \quad \theta_4]^T$ (rad); $\omega = \frac{d\theta}{dt} = [\omega_1 \quad \omega_2 \quad \omega_3 \quad \omega_4]^T$ (rad/s); $\xi = \frac{d^2\theta}{dt^2} = [\xi_1 \quad \xi_2 \quad \xi_3 \quad \xi_4]^T$ (rad/s^2); $u_M = [u_{M_1} \quad u_{M_2} \quad u_{M_3} \quad u_{M_4}]^T$ (Nm) is the vector of torques exerted by the servo motors ; $u_H = [u_{H_1} \quad u_{H_2} \quad u_{H_3} \quad u_{H_4}]^T$ (Nm) is the vector of torques exerted by the user.

The details of matrices in the Eq. (3) are provided in the appendix. The joint damping of joint i is expressed as follows [17], [18]:

$$D_i(\omega_i) = b_i\omega_i, \quad (i = 1,2,3,4), \quad (4)$$

where, b_i are coefficients of damping of joint i (i = 1, 2, 3, 4).

The force control in Eq. (3) contains two phases:

Phase 1: The user actively exert forces to signal the exoskeleton robot to generate the desired velocities.

Phase 2: The arm exoskeleton is actuated to assist the user motion. The feedback force and velocity controller contains two parts. The first part of the control is the force control which controls the feedback interaction forces on the links to track the desired feedback forces on the links. The second part of the control is the velocity control which controls the feedback velocities of joints to track the desired angular velocities of joints.

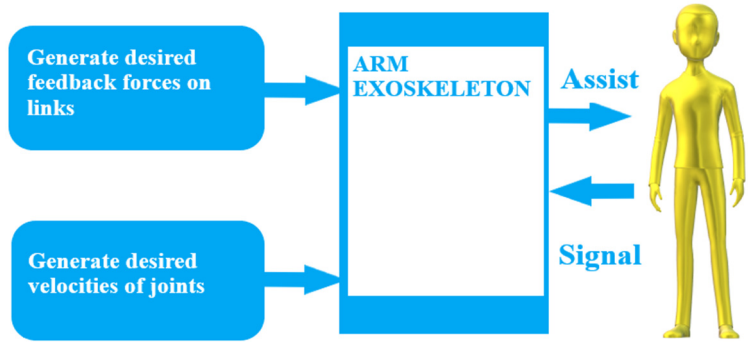

Fig. 2. Block diagram of the feedback force and velocity control

The block diagram of the feedback force and velocity control is explained in Fig. 2. In phase 1, the user exerts forces to signal the arm exoskeleton to generate the desired velocities. In phase 2, the desired feedback forces on the links are generated in Eq. (8). The desired angular velocities of the joints are based on Eq. (12).

The feedback forces on the links 1, 2, 3, 4 can be measured in reality. In numerical method, the user's forces exerted on the links are modeled in the Eqs. (5), (6):

$$F_{H_i} = \frac{\eta_{F_i}}{\sqrt{1+\eta_{F_i}^2}} F_{max_i} \text{ (N)}, \quad (5)$$

$$\eta_{F_i} = \frac{K_i l_i\left(\theta_{ds_i} - \theta_i\right) + B_i l_i \dfrac{d\left(\theta_{ds_i} - \theta_i\right)}{dt}}{F_{max_i}}, \quad i = 1, 2, 3, 4, \tag{6}$$

$$u_H = J_1^T R_1^0 \begin{bmatrix} F_{H_1} \\ 0 \\ 0 \end{bmatrix} + J_2^T R_2^0 \begin{bmatrix} 0 \\ F_{H_2} \\ 0 \end{bmatrix} + J_3^T R_3^0 \begin{bmatrix} 0 \\ F_{H_3} \\ 0 \end{bmatrix} + J_4^T R_4^0 \begin{bmatrix} 0 \\ 0 \\ F_{H_4} \end{bmatrix} \text{ (Nm)}, \tag{7}$$

where, K_i (N/m); B_i (Ns/m); l_i (m); $\theta_{ds} = [\theta_{ds_1} \quad \theta_{ds_2} \quad \theta_{ds_3} \quad \theta_{ds_4}]^T$ (rad); $\theta = [\theta_1 \quad \theta_2 \quad \theta_3 \quad \theta_4]^T$ (rad); F_{H_i} (N) is the user force; F_{max_i} (N) is the maximum user force on link i (i = 1, 2, 3, 4); $J_i = \left[\frac{\partial r_i}{\partial \theta_1} \quad \frac{\partial r_i}{\partial \theta_2} \quad \frac{\partial r_i}{\partial \theta_3} \quad \frac{\partial r_i}{\partial \theta_4}\right]$ is the Jacobian matrix; $r_i = [x_i \quad y_i \quad z_i]^T$ (m); R_i^0 is the rotation matrix; The details of matrices in the Eq. (7) are provided in the Appendix.

In phase 2, the desired feedback forces are generated to assist the user motion as follows [12], [13]:

$$F_{ds_i} = \alpha\left(\frac{d\theta_{ds_i}}{dt} - \frac{d\theta_i}{dt}\right) + \beta\left(\theta_{ds_i} - \theta_i\right) + \gamma G_i(\theta) \quad \text{(N)}, \tag{8}$$

where, α, β, γ are virtual coefficients; $G_i(\theta)$ (Nm) is the gravitational torque of link i (i = 1, 2, 3, 4).

The differences are as follows:

$$e_{F_i} = F_{ds_i} - F_{ms_i}, \tag{9}$$

where, F_{ms_i} is the measured feedback force on the link i (i = 1, 2, 3, 4).

In numerical method, the measured feedback forces are modeled as follows:

$$F_{ms_i} = P_1 F_d + P_2 F_{H_i}, \tag{10}$$

where, F_d, F_{H_i} are disturbances and the forces exerted by the human user, i (i = 1, 2, 3, 4), P_1, P_2 are the coefficients in the measurement.

The differences are utilized in the force control to actuate joints by using transposed Jacobian matrices as follows:

$$u_E = J_1^T R_1^0 \begin{bmatrix} e_{F_1} \\ 0 \\ 0 \end{bmatrix} + J_2^T R_2^0 \begin{bmatrix} 0 \\ e_{F_2} \\ 0 \end{bmatrix} + J_3^T R_3^0 \begin{bmatrix} 0 \\ e_{F_3} \\ 0 \end{bmatrix} + J_4^T R_4^0 \begin{bmatrix} 0 \\ 0 \\ e_{F_4} \end{bmatrix} \text{ (Nm)}. \tag{11}$$

The feedback force and velocity control is proposed as follows ([19], [20-23]):

$$u_C = H_F u_E + H_V(\omega_{ds} - \omega) \quad \text{(Nm)}, \tag{12}$$

where, H_F, H_V are the proportional gains of the feedback force control and velocity control, respectively $\omega_{ds} = [\omega_{ds_1} \quad \omega_{ds_2} \quad \omega_{ds_3} \quad \omega_{ds_4}]^T$ (rad/s); $\omega = [\omega_1 \quad \omega_2 \quad \omega_3 \quad \omega_4]^T$ (rad/s) is vector of the current angular velocities of the exoskeleton at joints 1, 2, 3, 4; $\omega_{ds_i} = \sigma F_{ms_i}$ (rad/s) is the desired angular velocity of joint i; σ (rad/s/N) is the coefficient of mobility of the desired motion.

The voltage of servo motor i, U_{S_i}, (i = 1, 2, 3, 4) are controlled following Eq. (13). In order to stabilize the voltages, the limited voltages are regulated as follows:

$$U_{S_i} = f\left(\eta_{U_{C_i}}\right) U_{Smax} \quad \text{(V)}, \tag{13}$$

where, $f(\eta_i) = \frac{\eta_{U_{C_i}}}{\sqrt{1+\eta^2_{U_{C_i}}}}$; $U_{S_{max}}$ (V); $\eta_{U_{C_i}} = \frac{u_{C_i}}{s_i}$ (Nm); $s_i = \mu_i \frac{U_{S_{max}}}{R_i} k_{t_i}$ (Nm); μ_i is the ratio between the output torque and the input torque of the gearbox of the servo motor i.

The relationship between the u_{M_i}, the output torque generated by servo motor i, and the voltage U_{s_i} ($i = 1, 2, 3, 4$), when $L_{ai} \approx 0$ and negligible, is as follows [24], [25]:

$$u_{M_i} = \mu_i . \left[U_{s_i} - k_{e_i} . \mu_i . \frac{d\theta_i}{dt} \right] . \frac{k_{t_i}}{R_{a_i}} \quad \text{(Nm)}, \tag{14}$$

where, $R_{a_i}(\Omega)$; k_{e_i} V/(rad/s); $\mu_i \frac{d\theta_i}{dt}$ (rad/s); L_{a_i} (H); I_{a_i}(A); k_{t_i} (Nm/A) are explained in the Table 2.

4. Optimal gains of the feedback force and velocity control

To find the optimal gains of the Feedback Force and Velocity control, the parameters of the arm exoskeleton are in Table 2.

Table 2. Parameters of a 4-DOF arm exoskeleton

Parameters of the arm exoskeleton	Values
Link length a_1, a_2, a_3, a_4 (m)	$a_1 = 0.2$, $a_2 = 0.3$, a_3 =0.4, $a_4 = 0.2$
Link mass m_1, m_2, m_3, m_4 (kg)	$m_1 = 0.3$, $m_2 = 0.5$, $m_3 = 0.3$, $m_4 = 0.5$
Distance l_1, l_2, l_3, l_4 (m)	$l_1 = l_2 = l_3 = l_4 = 0.2$
Virtual coefficients α (Ns/rad), β (N/rad), γ (1/m)	α = 0.5, β = 0.5, γ = 0.5
Viscousity damping coefficients b_1, b_2, b_3, b_4 (Nms/rad)	$b_1 = b_2 = b_3 = b_4 = 0.3$
Inertia moments of links I_L (kg.m^2)	I_L = diag[0.20,0.30,0.40,0.20]
Inertia moments of servo motors I_M (kg.m^2)	I_M= diag[0.80,0.50,0.40,0.60]
Supplied voltage $U_{S_{max}}$(V)	$U_{S_{max}} = 12$
Stiffness K_1, K_2, K_3, K_4 (N/m)	$K_1 = K_2 = K_3 = K_4 = 10000$
Damping B_1, B_2, B_3, B_4 (Ns/m)	$B_1 = B_2 = B_3 = B_4 = 100$
Maximum interaction forces on links (N)	F_{max_1}= 2, $F_{max_2} = 3$, $F_{max_3} = 2$, $F_{max_4} = 1$
Torque constant parameters k_{t_1}, k_{t_2}, k_{t_3}, k_{t_4} (Nm/A)	$k_{t_1} = 0.002$, $k_{t_2} = 0.003$, $k_{t_3} = 0.002$, $k_{t_4} = 0.001$
Back electro motive force (Voltage) constant parameters k_{e_1}, k_{e_2}, k_{e_3}, k_{e_4} (Vs/rad)	$k_{e_1} = k_{e_2} = k_{e_3} = k_{e_4} = 0.001$
Resistor parameters R_{a_1}, R_{a_2}, R_{a_3}, R_{a_4} (Ω)	$R_{a_1} = R_{a_2} = R_{a_3} = R_{a_4} = 3$
Ratio gearbox parameters μ_1, μ_2, μ_3, μ_4	$\mu_1 = \mu_2 = \mu_3 = \mu_4 = 250$
Proportional gain of the controller: $H_{F_{opt}}$, $H_{V_{opt}}$	Automatically optimized by BCMO
Maximum allowed torques s_1, s_2, s_3, s_4 (Nm)	$s_1 = 2$, $s_2 = 3$, $s_3 = 2$, $s_4 = 1$
The disturbance from outside environment F_d (N)	$F_d = 0.01\sin(100t)$
The coefficients of the disturbance in the measurements and user's force, respectively	$P_1 = 1$, $P_2 = -1$
The coefficient of mobility or admittance σ (rad/s/N)	$\sigma = -0.2$
Simulation time T (s)	$T = 20$

The desired angles and desired angular velocities of the joints are:

$$\begin{aligned} &\theta_{ds_1} = \theta_{ds_2} = \theta_{ds_3} = \theta_{ds_4} = 0.25 \quad \text{(rad)}, \\ &\omega_{ds_i} = -0.2F_{ms_i} \quad \text{(rad/s)}, \quad (i = 1,2,3,4). \end{aligned} \tag{15}$$

The initial positions and initial angular velocities of the joints are:

$$\theta_0 = [0 \quad 0 \quad 0 \quad 0] \text{ (rad)}, \\ \omega_0 = [0 \quad 0 \quad 0 \quad 0]^T \text{ (rad/s)}. \tag{16}$$

In the algorithm, the gains $H_{F_{opt}}$, $H_{V_{opt}}$ of the feedback force and velocity control will be optimized to minimize the root mean square of the error in the Eq. (17):

$$RMS(e_F) = \sqrt{\frac{1}{N}\sum_{i=1}^{N}\left(e_{F_4}^2\right)_i}. \tag{17}$$

In the algorithm, the initial values are $MaxGen = 10$, $N_P = 50$, $U_B = 500$, $L_B = 0$; the optimal function of BCMO is the$RMS(e_F)$. The optimized proportional gains of the feedback force and velocity control are: $H_F = 48$, $H_V = 394$. The optimal $RMS(e_F) = 0.47$ (N). The simulations of angles of joints and angular velocities of joints are carried out in Figs. 3, 4. The simulations of the feedback forces on the links are shown in Fig. 5.

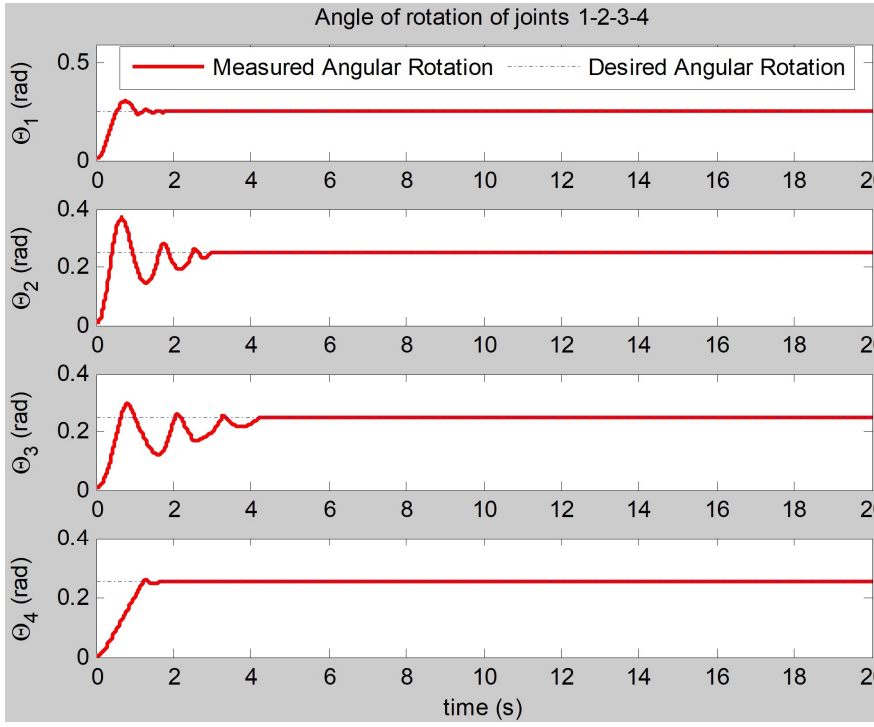

Fig. 3. The simulation of the angles of joints (rad) realized by the feedback force and velocity control

In case of the original control [12], the optimal gains of the original control obtained by BCMO are: $H_F = 81$, $H_P = 394$. The optimal root mean square of error is:$RMS(e_F) = 0.52$ (N). The simulation of angles of joints, angular velocities of joints, feedback forces on the links realized by original control are shown in Figs. 6, 7, 8.

In comparison, the feedback force and position control contains more oscillation in the feedback forces on the links than the feedback force and velocity control contains, and these oscillation in the feedback forces on the links can cause damages to the user. With the proposed feedback force and velocity control, the feedback force control has been improved in terms of fast response and less oscillation when generating safer feedback forces on the links.

ISSN PRINT 2351-5279, ISSN ONLINE 2424-4627

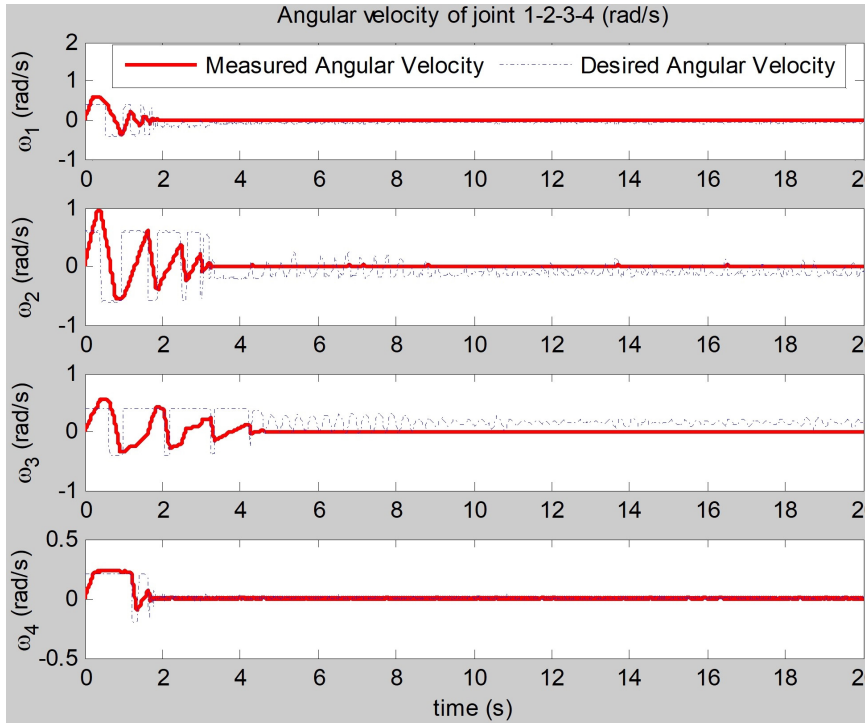

Fig. 4. The simulation of the angular velocities of joints (rad/s) realized by the feedback force and velocity control

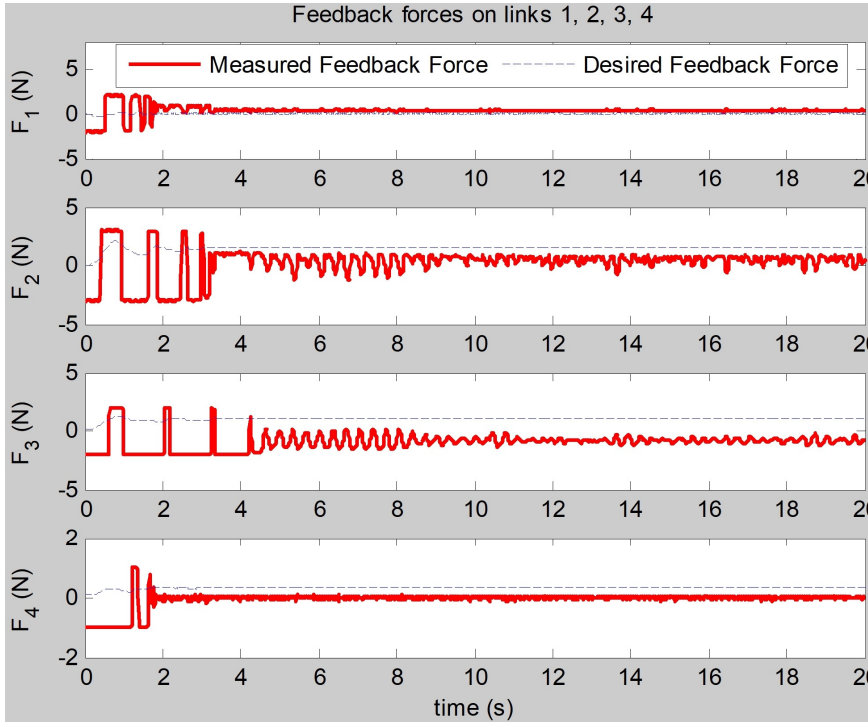

Fig. 5. The simulation of the feedback forces on the links (N) realized by the feedback force and velocity control

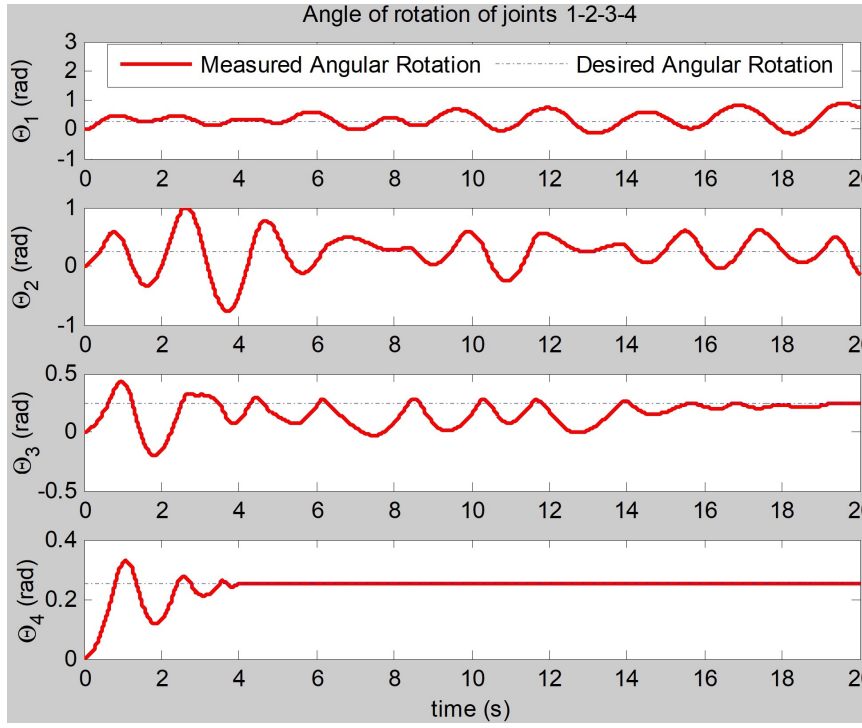

Fig. 6. The simulation of the angles of joints (rad) realized by the original control

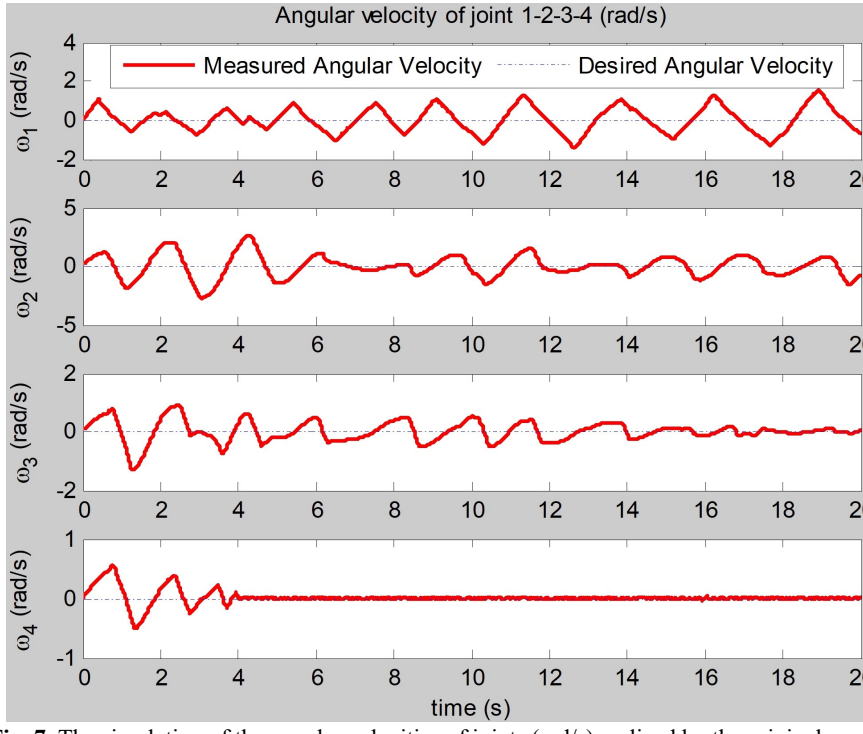

Fig. 7. The simulation of the angular velocities of joints (rad/s) realized by the original control

ISSN PRINT 2351-5279, ISSN ONLINE 2424-4627

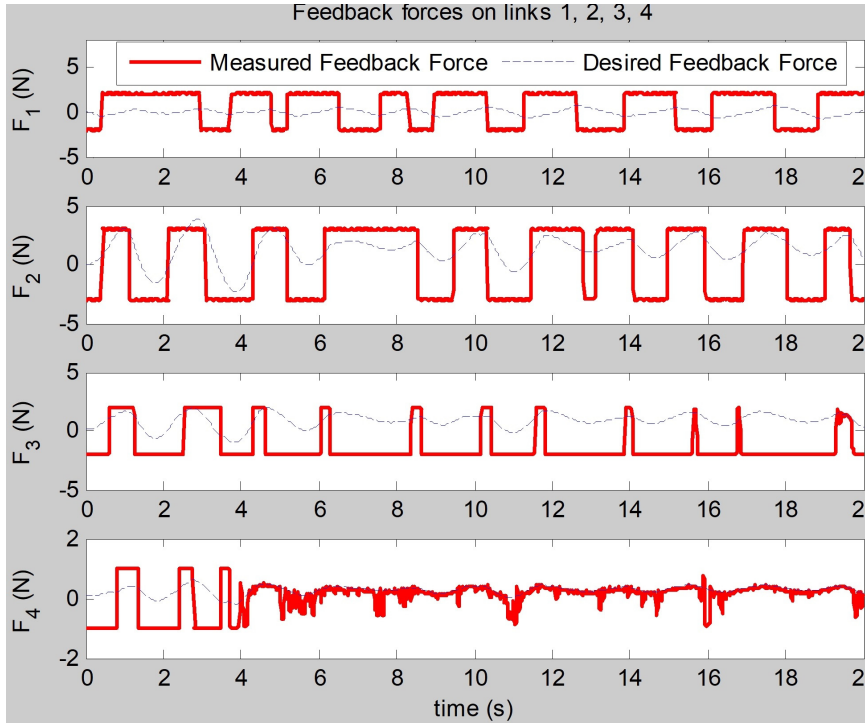

Fig. 8. The simulation of the feedback forces on the links (N) realized by the original control

5. Conclusions

In the paper, the feedback force and velocity control to regulate the better feedback forces on the links is realized and optimized by BCMO. The feedback force and velocity control aims at assisting user motions. When the user moves his arm, the arm exoskeleton is actuated to assist his motion. The numerical simulation shows that the feedback force and velocity control has achieved the safer feedback forces on the links in terms of fast response and less oscillation.

Acknowledgements

The paper is supported by Vietnam Academy of Science and Technology (VAST) under grant number CSCL03.03/23-24.

Data availability

The datasets generated during and/or analyzed during the current study are available from the corresponding author on reasonable request.

Author contributions

Thang Cao Nguyen: modelling, control design; Ngoc Tuan Nguyen: revise, check.

Conflict of interest

The authors declare that they have no conflict of interest.

References

[1] R. A. R. C. Gopura and K. Kiguchi, "Mechanical designs of active upper-limb exoskeleton robots: State-of-the-art and design difficulties," in *IEEE International Conference on Rehabilitation Robotics (ICORR)*, p. -, 2009.

[2] H. S. Lo and S. Q. Xie, "Exoskeleton robots for upper-limb rehabilitation: State of the art and future prospects," *Medical Engineering and Physics*, Vol. 34, No. 3, pp. 261–268, Apr. 2012, https://doi.org/10.1016/j.medengphy.2011.10.004

[3] J. L. Pons, *Wearable Robots: Biomechatronic Exoskeletons*. Wiley Online Library, 2008.

[4] Khairulanam and A. A. Al-Jumaily, "Active Exoskeleton Control Systems: State of the Art," in *International Symposium on Robotics and Intelligent Sensors 2012 (IRIS 2012)*, Vol. 41, pp. 988–994, 2012.

[5] E. Magrini and A. de Luca, "Hybrid force/velocity control for physical human-robot collaboration tasks," in *2016 IEEE/RSJ International Conference on Intelligent Robots and Systems (IROS)*, pp. 857–863, Oct. 2016, https://doi.org/10.1109/iros.2016.7759151

[6] C. Silawatchananai and M. Parnichkun, "Haptics control of an arm exoskeleton for virtual reality using PSO-based fixed structure H∞ control," *International Journal of Advanced Robotic Systems*, Vol. 16, No. 3, p. 172988141984919, May 2019, https://doi.org/10.1177/1729881419849198

[7] C. Silawatchananai and M. Parnichkun, "Force control of an upper limb exoskeleton for virtual reality using impedance control," in *IEEE International Conference on Robotics and Biomimetics*, pp. 2342–2347, 2011.

[8] H. Kazerooni, "Human robot interaction via the transfer of power and information signals," *IEEE Transactions on Systems, Man, Cybernetics*, Vol. 20, No. 2, pp. 450–463, 1990.

[9] H. Kazerooni, R. Steger, and L. Huang, "Hybrid control of the Berkeley lower extremity exoskeleton (BLEEX)," *The International Journal of Robotics Research*, Vol. 25, pp. 561–573, 2006.

[10] J. Tang, J. Zheng, and Y. Wang, "Direct force control of upper-limb exoskeleton based on fuzzy adaptive algorithm," *Journal of Vibroengineering*, Vol. 20, No. 1, pp. 636–650, 2018.

[11] T. C. Nguyen, M. Parnichkun, M. T. T. Phan, A. D. Nguyen, C. N. Pham, and H. N. Nguyen, "Force control of upper limb exoskeleton to support user movement," *Journal of Mechanical Engineering, Automation and Control Systems*, Vol. 1, No. 2, pp. 89–101, Dec. 2020, https://doi.org/10.21595/jmeacs.2020.21689

[12] T. C. Nguyen, A. D. Nguyen, M. Parnichkun, and M. T. T. Phan, "Feedback hybrid force and position control of an upper limb exoskeleton to support human movement," *Robotic Systems and Applications*, Vol. 3, No. 2, pp. 84–97, Dec. 2023, https://doi.org/10.21595/rsa.2023.23623

[13] H. J. Lee, K.-S. Kim, and S. Kim, "Generalized control framework for exoskeleton robots by interaction force feedback control," *International Journal of Control, Automation and Systems*, Vol. 19, No. 10, pp. 3419–3427, Jul. 2021, https://doi.org/10.1007/s12555-020-0097-2

[14] T. L. Duc, Q. H. Nguyen, and H. N. Xuan, "Balancing composite motion optimization," *Information Sciences*, Vol. 520, pp. 250–270, 2020.

[15] M. W. Spong, S. Hutchinson, and M. Vidyasagar, *Robot Dynamics and Control*. Wiley, 2004.

[16] D. Sanh, D. Phong, and D. D. Khoa, "Motion of mechanical system with non-ideal constraints," *Vietnam Journal of Mechanics*, Vol. 35, No. 2, pp. 157–167, 2013.

[17] T. Tjahjowidodo, F. Al-Bender, and H. Brussel, "Friction identification and compensation in a dc motor," *IFAC Proc Vol (IFAC-PapersOnline)*, Vol. 38, No. 1, pp. 554–559, 2005.

[18] H. Liu, Y. Liu, and M. Jin, "An experimental study on Cartesian impedance control for a joint torque-based manipulator," *Adv Robot*, Vol. 22, No. 11, pp. 1155–1180, 2008.

[19] R. P. Borase, D. K. Maghade, S. Y. Sondkar, and S. N. Pawar, "A review of PID control, tuning methods and applications," *International Journal of Dynamics and Control*, Vol. 9, No. 2, pp. 818–827, Jul. 2020, https://doi.org/10.1007/s40435-020-00665-4

[20] G. Liang, W. Ye, and Q. Xie, "PID control for the robotic exoskeleton: application to lower extremity rehabilitation," in *IEEE International Conference on Mechatronics and Automation*, 2012.

[21] S. Oh, E. Baek, S.-K. Song, S. Mohammed, D. Jeon, and K. Kong, "A generalized control framework of assistive controllers and its application to lower limb exoskeletons," *Robotics and Autonomous Systems*, Vol. 73, pp. 68–77, 2015.

[22] M. Hessinger, M. Pingsmann, J. C. Perry, R. Werthschutzky, and M. Kupnik, "Hybrid position/force control of an upper-limb exoskeleton for assisted drilling," in *2017 IEEE/RSJ International Conference*

on Intelligent Robots and Systems (IROS), pp. 1824–1829, Sep. 2017, https://doi.org/10.1109/iros.2017.8205997

[23] V. Avilés, O. F. Avilés, J. Aponte, O. I. Caldas, and M. F. Mauledoux, "Performance analysis between a hybrid force/position and conventional controllers for a wrist exoskeleton," *Archives of Control Sciences*, Vol. 32, pp. 409–427, 2022.

[24] S. Centinkunt, *Mechatronics*. John Wiley & Sons, Inc, 2007.

[25] D. G. Alciatore and M. B. Histand, *Introduction to Mechatronics and Measurement Systems*. New York: McGraw Hill, 2007.

Appendix

In the nonlinear dynamic equation as shown in Eq. (3), we define θ_1, θ_2, θ_3, θ_4 are angles of rotation of joint 1, 2, 3, 4, respectively. ω_1, ω_2, ω_3, ω_4 are angular velocities of joint 1, 2, 3, 4, respectively. m_1, m_2, m_3, m_4 are masses of links 1, 2, 3, 4, respectively. a_1, a_2, a_3, a_4 are lengths of links 1, 2, 3, 4, respectively.

And we denote:

$$A_2 = a_2\sin\theta_2, \quad B_2 = a_2\cos\theta_2,$$
$$A_3 = a_3\sin(\theta_2+\theta_3), \quad B_3 = a_3\cos(\theta_2+\theta_3),$$
$$A_4 = a_4\sin(\theta_2+\theta_3+\theta_4), \quad B_4 = a_4\cos(\theta_2+\theta_3+\theta_4),$$
$$s_3 = \sin\theta_3, \quad c_3 = \cos\theta_3, \quad s_4 = \sin\theta_4, \quad c_4 = \cos\theta_4,$$
$$s_{34} = \sin(\theta_3+\theta_4), \quad c_{34} = \cos(\theta_3+\theta_4),$$
$$s_{23} = \sin(\theta_2+\theta_3), \quad c_{23} = \cos(\theta_2+\theta_3),$$
$$s_{234} = \sin(\theta_2+\theta_3+\theta_4), \quad c_{234} = \cos(\theta_2+\theta_3+\theta_4).$$

The detail elements of the matrix of inertia moments of joints are:

$$M = \begin{bmatrix} a_{11} & a_{12} & a_{13} & a_{14} \\ a_{21} & a_{22} & a_{23} & a_{24} \\ a_{31} & a_{32} & a_{33} & a_{34} \\ a_{41} & a_{42} & a_{43} & a_{44} \end{bmatrix} + I_L + I_M \quad (\text{kg.m}^2),$$

where:

$$a_{11} = m_1a_1^2 + m_2(a_1^2 + A_2^2) + m_3(a_1^2 + (A_2+A_3)^2) + m_4(a_1^2 + (A_2+A_3+A_4)^2),$$
$$a_{22} = m_2a_2^2 + m_3(a_2^2 + a_3^2 + 2a_2a_3c_3) + m_4(a_2^2 + a_3^2 + a_4^2 + 2a_2a_3c_3 + 2a_2a_4c_{34} + 2a_3a_4c_4),$$
$$a_{33} = m_3a_3^2 + m_4(a_3^2 + a_4^2 + 2a_3a_4c_4),$$
$$a_{44} = m_4a_4^2,$$
$$a_{12} = a_1\big(m_2B_2 + m_3(B_2+B_3) + m_4(B_2+B_3+B_4)\big),$$
$$a_{13} = a_1\big(m_3B_3 + m_4(B_3+B_4)\big),$$
$$a_{14} = m_4B_4a_1,$$
$$a_{23} = m_3a_3^2 + m_3a_2a_3c_3 + m_4(a_3^2 + a_4^2 + a_2a_3c_3 + a_2a_4c_{34} + 2a_3a_4c_4),$$
$$a_{24} = m_4a_4^2 + m_4a_2a_4c_{34} + m_4a_3a_4c_4,$$
$$a_{34} = m_4a_4^2 + m_4a_3a_4c_4, \quad a_{ij} = a_{ji}, \quad (i,j = 1,2,3,4).$$

The matrix of the inertial moment of the links 1, 2, 3, 4 is:

$$I_L = \begin{bmatrix} I_{L11} & 0 & 0 & 0 \\ 0 & I_{L22} & 0 & 0 \\ 0 & 0 & I_{L33} & 0 \\ 0 & 0 & 0 & I_{L44} \end{bmatrix} \quad (\text{kg.m}^2).$$

The matrix of the inertial moment of the servo motors at joints 1, 2, 3, 4 is:

$$I_M = \begin{bmatrix} I_{M11} & 0 & 0 & 0 \\ 0 & I_{M22} & 0 & 0 \\ 0 & 0 & I_{M33} & 0 \\ 0 & 0 & 0 & I_{M44} \end{bmatrix} \quad (\text{kg.m}^2).$$

The detail elements of the vector of Coriolis and centrifugal forces are:

$$C = [C_1 \quad C_2 \quad C_3 \quad C_4]^T \quad (\text{kg.m}^2/\text{s}^2),$$

where:

$$C_1 = \left(2m_2A_2B_2 + 2m_3(A_2 + A_3)(B_2 + B_3) + 2m_4\sum_{i=2}^{4}A_i\sum_{i=2}^{4}B_i\right)\omega_1\omega_2$$
$$+\left(2m_3(A_2 + A_3)B_3 + 2m_4\sum_{i=2}^{4}A_i\,(B_3 + B_4)\right)\omega_1\omega_3 + 2m_4\sum_{i=2}^{4}A_i\,B_4\omega_1\omega_4$$
$$-a_1\left(m_2A_2 + m_3(A_2 + A_3) + m_4\sum_{i=2}^{4}A_i\right)\omega_2^2 - a_1\left(m_3A_3 + m_4\sum_{i=3}^{4}A_i\right)\omega_3^2$$
$$-a_1m_4A_4\omega_4^2 - 2a_1\left(m_3A_3 + m_4\sum_{i=3}^{4}A_i\right)\omega_2\omega_3 - 2a_1m_4A_4(\omega_2 + \omega_3)\omega_4,$$

$$C_2 = -(m_3a_2a_3s_3 + m_4a_2a_3s_3 + m_4a_2a_4s_{34})(2\omega_2\omega_3 + {\omega_3}^2)$$
$$-(m_4a_2a_4s_{34} + m_4a_3a_4s_4)(2\omega_2\omega_4 + 2\omega_3\omega_4 + {\omega_4}^2)$$
$$-\left(m_2A_2B_2 + m_3(A_2 + A_3)(B_2 + B_3) + m_4\sum_{i=2}^{4}A_i\sum_{i=2}^{4}B_i\right){\omega_1}^2,$$

$$C_3 = -m_4a_3a_4S_4(2\omega_2\omega_4 + 2\omega_3\omega_4 + {\omega_4}^2) - \left(m_3(A_2 + A_3)B_3 + m_4\sum_{i=2}^{4}A_i\,(B_3 + B_4)\right){\omega_1}^2$$
$$+(m_3a_2a_3s_3 + m_4a_2a_3s_3 + m_4a_2a_4s_{34}){\omega_2}^2,$$

$$C_4 = -m_4\sum_{i=2}^{4}A_i\,B_4{\omega_1}^2 + (m_4a_2a_4s_{34} + m_4a_3a_4s_4){\omega_2}^2 + 2\,m_4a_3a_4s_4\omega_2\omega_3$$
$$+ m_4a_3a_4s_4{\omega_3}^2.$$

The detail elements of vector of gravitational forces are:

$$G(\theta) = [G_1 \quad G_2 \quad G_3 \quad G_4]^T \quad (\text{kg.m}^2/\text{s}^2),$$

where, $G_1 = 0$; $G_2 = m_2gA_2 + m_3g(A_2 + A_3) + m_4g(A_2 + A_3 + A_4)$; $G_3 = m_3gA_3 + m_4g(A_3 + A_4)$; $G_4 = m_4gA_4$.

The rotation matrices and the Jacobian matrices of joints 1, 2, 3, 4 are:

– Joint 1:

$$R_1^0 = A_1^0(1{:}3,1{:}3) = \begin{bmatrix} -s_1 & 0 & c_1 \\ c_1 & 0 & s_1 \\ 0 & 1 & 0 \end{bmatrix}, \tag{18}$$

$$r_1 = \begin{bmatrix} l_1 c_1 \\ l_1 s_1 \\ 0 \end{bmatrix}, \quad J_1 = \begin{bmatrix} \frac{\partial r_1}{\partial \theta_1} & \frac{\partial r_1}{\partial \theta_2} & \frac{\partial r_1}{\partial \theta_3} & \frac{\partial r_1}{\partial \theta_4} \end{bmatrix} = \begin{bmatrix} -l_1 s_1 & 0 & 0 & 0 \\ l_1 c_1 & 0 & 0 & 0 \\ 0 & 0 & 0 & 0 \end{bmatrix}. \tag{19}$$

From Eqs. (18) and (19), one has:

$$J_1^T R_1^0 = \begin{bmatrix} l_1 & 0 & 0 \\ 0 & 0 & 0 \\ 0 & 0 & 0 \\ 0 & 0 & 0 \end{bmatrix}.$$

– Joint 2:

$$R_2^0 = R_1^0 . R_2^1 = A_1^0(1:3,1:3) . A_2^1(1:3,1:3) = A_2^0(1:3,1:3) = \begin{bmatrix} -s_1 s_2 & -s_1 c_2 & c_1 \\ c_1 s_2 & c_1 c_2 & s_1 \\ -c_2 & s_2 & 0 \end{bmatrix}, \tag{20}$$

$$r_2 = \begin{bmatrix} -l_2 s_1 s_2 + a_1 c_1 \\ l_2 c_1 s_2 + a_1 s_1 \\ -l_2 c_2 \end{bmatrix},$$

$$J_2 = \begin{bmatrix} \frac{\partial r_2}{\partial \theta_1} & \frac{\partial r_2}{\partial \theta_2} & \frac{\partial r_2}{\partial \theta_3} & \frac{\partial r_2}{\partial \theta_4} \end{bmatrix} = \begin{bmatrix} -l_2 c_1 s_2 - a_1 s_1 & -l_2 s_1 c_2 & 0 & 0 \\ -l_2 s_1 s_2 + a_1 c_1 & l_2 c_1 c_2 & 0 & 0 \\ 0 & l_2 s_2 & 0 & 0 \end{bmatrix}. \tag{21}$$

From Eqs. (20) and (21), one has:

$$J_2^T R_2^0 = \begin{bmatrix} a_1 s_2 & a_1 c_2 & -l_2 s_2 \\ 0 & l_2 & 0 \\ 0 & 0 & 0 \\ 0 & 0 & 0 \end{bmatrix}.$$

– Joint 3:

$$\begin{aligned} R_3^0 &= R_1^0 . R_2^1 . R_3^2 = A_1^0(1:3,1:3) . A_2^1(1:3,1:3) . A_3^2(1:3,1:3) \\ &= A_3^0(1:3,1:3) = \begin{bmatrix} -s_1 s_{23} & -s_1 c_{23} & c_1 \\ c_1 s_{23} & c_1 c_{23} & s_1 \\ -c_{23} & s_{23} & 0 \end{bmatrix}, \end{aligned} \tag{22}$$

$$r_3 = \begin{bmatrix} -s_1(a_2 s_2 + l_3 s_{23}) + a_1 c_1 \\ c_1(a_2 s_2 + l_3 s_{23}) + a_1 s_1 \\ -a_2 c_2 - l_3 c_{23} \end{bmatrix},$$

$$\begin{aligned} J_3 &= \begin{bmatrix} \frac{\partial r_3}{\partial \theta_1} & \frac{\partial r_3}{\partial \theta_2} & \frac{\partial r_3}{\partial \theta_3} & \frac{\partial r_3}{\partial \theta_4} \end{bmatrix} \\ &= \begin{bmatrix} -c_1(a_2 s_2 + l_3 s_{23}) - a_1 s_1 & -s_1(a_2 c_2 + l_3 c_{23}) & -s_1 l_3 c_{23} & 0 \\ -s_1(a_2 s_2 + l_3 s_{23}) + a_1 c_1 & c_1(a_2 c_2 + l_3 c_{23}) & c_1 l_3 c_{23} & 0 \\ 0 & a_2 s_2 + l_3 s_{23} & l_3 s_{23} & 0 \end{bmatrix}. \end{aligned} \tag{23}$$

From Eqs. (22) and (23), one has:

$$J_3^T R_3^0 = \begin{bmatrix} a_1 s_{23} & a_1 c_{23} & -a_2 s_2 - l_3 s_{23} \\ a_2 s_3 & a_2 c_3 + l_3 & 0 \\ 0 & l_3 & 0 \\ 0 & 0 & 0 \end{bmatrix}.$$

– Joint 4:

$$R_4^0 = R_1^0.R_2^1.R_3^2.R_4^3 = A_1^0(1:3,1:3).A_2^1(1:3,1:3).A_3^2(1:3,1:3).A_4^3(1:3,1:3)$$
$$= A_4^0(1:3,1:3) = \begin{bmatrix} c_1 & -s_1 s_{234} & -s_1 c_{234} \\ s_1 & c_1 s_{234} & c_1 c_{234} \\ 0 & -c_{234} & s_{234} \end{bmatrix}, \quad (24)$$

$$r_4 = \begin{bmatrix} -s_1(a_2 s_2 + a_3 s_{23} + l_4 s_{234}) + a_1 c_1 \\ c_1(a_2 s_2 + a_3 s_{23} + l_4 s_{234}) + a_1 s_1 \\ -a_2 c_2 - a_3 c_{23} - l_4 c_{234} \end{bmatrix},$$

$$J_4 = \begin{bmatrix} \frac{\partial r_4}{\partial \theta_1} & \frac{\partial r_4}{\partial \theta_2} & \frac{\partial r_4}{\partial \theta_3} & \frac{\partial r_4}{\partial \theta_4} \end{bmatrix}$$
$$= \begin{bmatrix} -c_1(a_2 s_2 + a_3 s_{23} + l_4 s_{234}) - a_1 s_1 & -s_1(a_2 c_2 + a_3 c_{23} + l_4 c_{234}) \\ -s_1(a_2 s_2 + a_3 s_{23} + l_4 s_{234}) + a_1 c_1 & c_1(a_2 c_2 + a_3 c_{23} + l_4 c_{234}) \\ 0 & a_2 s_2 + a_3 s_{23} + l_4 s_{234} \\ -s_1(a_3 c_{23} + l_4 c_{234}) & -s_1 l_4 c_{234} \\ c_1(a_3 c_{23} + l_4 c_{234}) & c_1 l_4 c_{234} \\ a_3 s_{23} + l_4 s_{234} & l_4 s_{234} \end{bmatrix}. \quad (25)$$

From (32) and (33), one has:

$$J_4^T R_4^0 = \begin{bmatrix} -a_2 s_2 - a_3 s_{23} - l_4 s_{234} & a_1 s_{234} & a_1 c_{234} \\ 0 & a_2 s_{34} + a_3 s_4 & l_4 + a_3 c_4 + a_2 c_{34} \\ 0 & a_3 s_4 & l_4 + a_3 c_4 \\ 0 & 0 & l_4 \end{bmatrix}.$$

Thang Cao Nguyen received his B.E. degree in Mechanical Engineering from Hanoi University of Science and Technology (HUST), Vietnam, in 2003. He received Master of Engineering degree in Mechatronics from Asian Institute of Technology (AIT), Bangkok, Thailand in 2009. He received his Ph.D. in Engineering Mechanics from Graduate University of Science and Technology (GUST), Vietnam, in 2020. He is currently working at Institute of Mechanics, Vietnam Academy of Science and Technology, Hanoi, Vietnam. His research interests are Robotics, Control, and Vibration.

Ngoc Tuan Nguyen received his B.S and M.S degrees in civil engineering from University of Civil Engineering, Hanoi, Vietnam, in 2005 and 2010, respectively. He is currently pursuing a Ph.D. degree in mechanical engineering at Graduate University of Science and Technology (GUST), Vietnam. His research interests include vibration and control of bridges.